Available online at www.sciencedirect.com

SCIENCE DIRECT

Developmental Biology 284 (2005) 72 – 83

DEVELOPMENTAL BIOLOGY

www.elsevier.com/locate/ydbio

Ablation of the secondary heart field leads to tetralogy of Fallot and pulmonary atresia

Cary Ward[a], Harriett Stadt[b], Mary Hutson[b], Margaret L. Kirby[b,*]

[a]*Department of Medicine (Cardiology), Duke University Medical Center, Durham, NC 27710, USA*
[b]*Department of Pediatrics (Neonatology), NeonatalPerinatal Research Institute, Duke University Medical Center, Durham, NC 27710, USA*

Received for publication 4 February 2005, revised 22 April 2005, accepted 4 May 2005
Available online 9 June 2005

Abstract

Recent studies in chick and mouse embryos have identified a previously unrecognized secondary heart field (SHF), located in the ventral midline splanchnic mesenchyme, which provides additional myocardial cells to the outflow tract as the heart tube lengthens during cardiac looping. In order to further delineate the contribution of this secondary myocardium to outflow development, we labeled the right SHF of Hamburger–Hamilton (HH) stage 14 chick embryos via microinjection of DiI/rhodamine and followed the fluorescently labeled cells over a 96-h time period. These experiments confirmed the movement of the SHF into the outflow and its spiraling migration distally, with the right side of the SHF contributing to the left side of the outflow. In contrast, when the right SHF was labeled at HH18, the fluorescence was limited to the caudal wall of the lengthening aortic sac. We then injected a combination of DiI and neutral red dye, and ablated the SHF in HH14 or 18 chick embryos. Embryos were allowed to develop until day 9, and harvested for assessment of outflow alignment. Of the embryos ablated at HH14, 76% demonstrated cardiac defects including overriding aorta and pulmonary atresia, while none of the sham-operated controls were affected. In addition, the more severely affected embryos demonstrated coronary artery anomalies. The embryos ablated at HH18 also manifested coronary artery anomalies but maintained normal outflow alignment. Therefore, the myocardium added to the outflow by the SHF at earlier stages is required for the elongation and appropriate alignment of the outflow tract. However, at later stages, the SHF contributes to the smooth muscle component of the outflow vessels above the pulmonary and aortic valves which is important for the development of the coronary artery stems. This work suggests a role for the SHF in a subset of congenital heart defects that have overriding aorta and coronary artery anomalies, such as tetralogy of Fallot and double outlet right ventricle.

Keywords: Secondary heart field; Pulmonary atresia; Ablation; Heart development; Conotruncal malformations

Introduction

Elongation of the midline heart tube is an important morphological process during formation of a four-chambered heart. Elongation provides the length that the tube needs for convergence of the inflow and outflow ends, and subsequently for the outflow tract to wedge between the right and left atrioventricular valves. Wedging is an important step because it brings the pulmonary trunk and aorta into the correct alignment with the right and left ventricular outlets, respectively. Failure of wedging leads to congenital heart malformations like tetralogy of Fallot and double outlet right ventricle (Yelbuz et al., 2002).

Several labs described the existence of a “secondary” or “anterior” heart field that serves as a source of myocardial cells to lengthen the outflow end of the tubular heart (Kelly et al., 2001; Mjaatvedt et al., 2001; Waldo et al., 2001). The secondary heart field (SHF) is located in the mesenchyme of the ventral pharynx between the inflow and outflow tracts. After neural crest ablation in the chick embryo, the myocardium is not added from the secondary heart field and the hearts have malaligned outflow tracts (Yelbuz et al., 2002; Waldo et al., 2005b).

* Corresponding author. Bell Building, Room 157, Box 3179, Neonatology, DUMC, Durham, NC 27712, USA. Fax: +1 919 668 1599.
E-mail address: mlkirby@duke.edu (M.L. Kirby).

0012-1606/$ - see front matter © 2005 Elsevier Inc. All rights reserved.
doi:10.1016/j.ydbio.2005.05.003

Ablation of the cardiac neural crest (mid-otic placode to somite 3 in chick embryos) results in cardiac defects, most commonly persistent truncus arteriosus (PTA). These PTAs are also malaligned since the truncus originates predominately from the right ventricle. In the neural-crest-ablated embryos that do not develop PTA, there are other defects of cardiac outflow alignment, namely, double outlet right ventricle and tetralogy of Fallot (Kirby et al., 1983) The alignment defects in addition to problems with septation suggest two separate anomalous processes seen after neural crest ablation. Further experiments with HIRA, a chromosomal remodeling gene expressed in neural crest cells, demonstrated that the malalignment of the outflow tract after neural crest ablation could indeed be separated from the septation defect, as embryos treated with antisense oligonucleotides to HIRA developed PTAs with normal alignment (Farrell et al., 1999a,b, 2001). Although the septation defect could be easily explained by the absence of the neural crest cells responsible for the formation of the aorticopulmonary septum, the origin of the alignment defect required further investigation. In a recent study, Yelbuz et al. (2002) proposed that the length of the outflow tract was affected by neural crest ablation. Using videocinephotography, scanning electron microscopy, and histological sections to assess outflow morphology, neural-crest-ablated embryos were found to have malpositioning of the inflow and outflow limbs, a diminished inner curvature, and a straighter and ventrally displaced outflow limb, all of which were consistent with a shorter outflow tract (Yelbuz et al., 2002). The reduced length was thought to be the result of a decreased contribution from the secondary heart field, an area of ventral midline splanchnic mesenchyme known to add myocardium to the developing outflow tract. HNK1 staining of neural-crest-ablated embryos at Hamburger–Hamilton (HH) stage 16 demonstrated drastically reduced migration of cells from the SHF into the developing outflow (Cai et al., 2003; Kelly et al., 2001; Mjaatvedt et al., 2001; Yelbuz et al., 2002). We therefore hypothesized that failure of cells to be added to the outflow tract from the SHF may be responsible for the defects of cardiac outflow alignment seen after neural crest ablation, since the shorter outflow tract is unable to undergo the rotation necessary for appropriate alignment of the aorta and pulmonary trunk with their respective ventricles.

To further investigate the role of the SHF in formation of the outflow tract, we labeled the SHF in HH14 chick embryos prior to its addition to the outflow tract and monitored the movement of the marked cells. These data confirmed the movement of the SHF into the developing outflow tract and also demonstrated that the right SHF spirals behind and to the left side of the conotruncal junction within the inner curvature. We then used a nitrogen-dye laser to ablate the right SHF of HH14 chick embryos. Defects of cardiac outflow alignment, as well as stenotic or atretic pulmonary trunks were found, confirming a role for the SHF in the appropriate alignment of the outflow, as well as a role for the right SHF in formation of the pulmonary (left) side of the outflow. We also performed labeling experiments as well as ablations of the right SHF in older HH18 embryos in which the myocardium of the SHF has already been added. These embryos demonstrated normal outflow alignment, confirming that the myocardial addition from the SHF is complete by HH18. Of note, the embryos ablated at HH18, as well as those most severely affected by ablations at HH14, possessed coronary artery anomalies. Other work in our laboratory demonstrates that, at later stages, the SHF adds smooth muscle to the developing outflow tract (Waldo et al., 2005a). The coronary artery anomalies seen in SHF-ablated embryos suggest that this smooth muscle addition is important for correct formation of the coronary artery stems.

Materials and methods

Embryos

Fertilized Ross Hubert chicken eggs (Goldkist Hatchery, Siler City, NC) were incubated at 37°C and 70% relative humidity until they reached the desired Hamburger–Hamilton stage (Hamburger and Hamilton, 1951). For shell-less cultures, embryos were transferred to hexagonal polycarbonate weigh boats which were placed in 15-cm Petri dishes with 0.5 cm of distilled water in the bottom. These were reincubated at 37°C and 70% relative humidity.

In situ hybridization and sectioning of stained embryos

An Nkx2.5 digoxygenin-labeled riboprobe was generated from a 221-bp fragment of the chick Nkx2.5 cDNA as previously described (Waldo et al., 2001). Whole mount in situ hybridization was carried out using the protocol described by Wilkinson (1992). After examination and documentation of whole mount staining, the embryos were embedded in paraffin, sectioned transversely at 12 μm, and mounted.

Microinjections

HH14 or 18 chick embryos were placed in shell-less culture and back-injected with green tissue marking dye (Triangle Biomedical Services) for better visualization of the pharynx. For the labeling experiments, DiI (Molecular Probes) was dissolved in DMSO at a concentration of 2.5 mg/ml. Tetramethylrhodamine-succinyl ester (TAMRA-SE, Molecular Probes) or carboxyfluorescein diacetate (CFSE, Molecular Probes) was dissolved in 100% ethanol at a concentration of 10 mg/ml. DiI and TAMRA-SE were then diluted 1:1:10 with normal saline. Pulled capillaries were used to inject approximately 1–2 nl of the diluted DiI/TAMRA-SE mixture into the right SHF. The injected embryos were incubated at 37°C and 70% relative humidity

until the desired time points of 24, 48, or 96 h after the injection. After examination and documentation of whole mount fluorescence, the embryos were fixed in 4% phosphate-buffered paraformaldehyde (PFA) for 24 h at 4°C. The embryos were processed for paraffin embedding, sectioned, and double immunostained for rhodamine and myocardium (MF20).

SHF ablations

DiI was dissolved as described above. Neutral red was dissolved in normal saline at a concentration of 0.4%. Using the techniques described above, neutral red alone or a mixture of neutral red plus DiI was microinjected into the right SHF of HH14 or HH18 chick embryos. Ablations were performed using a pulsed nitrogen-dye laser both in shell-less culture and in ovo. Sham-operated embryos were injected as described above and returned to the incubator. Ablated and sham embryos were incubated at 37°C and 70% relative humidity until the desired developmental stage. A series of embryos was allowed to develop until day 9 to determine the gross morphology of the fully septated heart. Hearts were harvested and immersion fixed in 10% formalin overnight. After examination and documentation of gross morphology, hearts were embedded in paraffin, sectioned, and mounted. Sections were stained with 0.5% thionine or hematoxylin and eosin.

Sytox green staining

Ablation of the SHF was performed as described above. The embryos were incubated for 1 h at 37°C and harvested in normal saline. Embryos were then stained in Sytox Green (1 μM, Molecular Probes) to label the laser-damaged SHF for 10 min. After examination and documentation of whole mount staining, embryos were fixed in 4% PFA for 10 min at 4°C. The embryos were then taken through a series of sucrose gradients, embedded in OCT, and cryosectioned.

Immunohistochemistry

SHF-ablated and sham-operated embryos were harvested at HH25/26, embedded in paraffin and sectioned at 8 μm. The sections were incubated as described previously (Waldo et al., 1996, 1998). HNK-1 (obtained from American Type Culture Collection) was visualized with Alexa 488 goat anti-mouse IgG conjugate (Molecular Probes) as reported previously (Waldo et al., 1996, 1998). MF20 was obtained from the Developmental Studies Hybridoma Bank developed under the auspices of NICHD and maintained by the University of Iowa, Department of Biological Sciences, Iowa City, IA. MF20 was visualized with Alexa 568 goat anti-mouse IgG conjugate. For the staining with factor-VIII-related antigen, SHF-ablated embryos were harvested at day 9 of development, fixed in Serra's solution, embedded in paraffin, and incubated as described previously (Ribatti et al., 1999). Antibody to factor-VIII-related antigen was obtained from DakoCytomation and used at a 1:250 dilution. The rabbit ABC Elite kit (Vector) was used for the secondary reaction with DAB visualization. The preparations were counter-stained with hematoxylin (Anatech, Battle Creek, MI).

Results

NKX2.5 expression in the developing heart and SHF

In order to better delineate the putative boundaries of the SHF, we performed in situ hybridization of Nkx2.5 (Fig. 1), a transcription factor known to be expressed in early myocardial precursor cells as well as the SHF (Waldo et al., 2001), at HH12–24 (Hamburger and Hamilton, 1951). At all stages, Nkx2.5 was expressed throughout the length of the heart tube (Fig. 1A). At HH12, extracardiac Nkx2.5 expression was notable in ventral pharyngeal mesenchyme both cranial and caudal to the junction of the outflow tract with the ventral pharynx (Figs. 1A–C). Nkx2.5 expression caudal to the connection of the outflow tract with the body wall, which represents the SHF, extended to the juncture of the inflow portion of the linear heart tube with the body wall. Diffuse expression was maintained at HH14 (Figs. 1D–F), as the linear heart tube proceeded with looping. At HH16, the Nkx2.5 expression increased in intensity in the SHF, but disappeared from the region cranial to the outflow (Fig. 1G). At HH18 (Figs. 1H and I), the amount of Nkx2.5 expression decreased in the region caudal to the outflow and was seen only in the area surrounding the attachment of the outflow with the ventral pharynx. This pattern of limited Nkx2.5 expression was unchanged at later stages up to HH24 (data not shown). The decrease in the size of the area of Nkx2.5 expression caudal to the outflow starting at HH18 coincided with the decrease in addition of cardiac precursor cells to the developing outflow tract from the SHF (Waldo et al., 2001), suggesting that the addition of myocardium may be complete by HH18 since the pattern remained unchanged at later stages.

The right side of the SHF contributes to the left side of the outflow myocardium

In order to better understand the mechanics of the addition of myocardial cells from the SHF to the developing outflow, we performed labeling experiments using DiI/rhodamine. Because the chick embryo lies on its right side after HH13, the left side is not reliably accessible for physical marking; thus, all of the marking experiments were done in the right SHF. The right side of the SHF of HH14 chick embryos in shell-less culture was microinjected with DiI/rhodamine, and fluorescence followed at 4-h intervals to 24, 48, and 96 h. After 24 h, the DiI/rhodamine-labeled cells migrated into the distal caudal outflow myocardium (Figs. 2A, B). At 48 h, labeled cells were seen in the caudal left

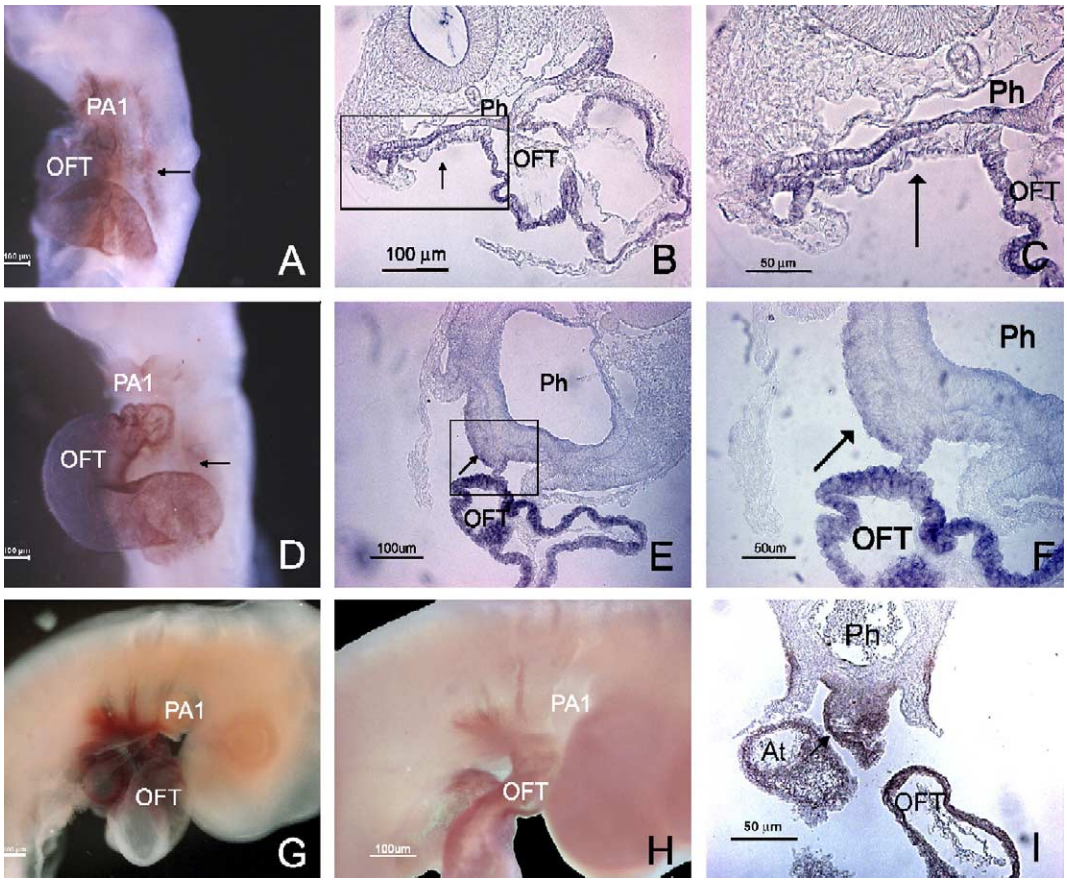

Fig. 1. Nkx2.5 expression in the developing heart and SHF. (A) In situ hybridization of Nkx2.5 in an HH12 embryo demonstrating expression in the heart tube and in the ventral pharynx surrounding and caudal to the juncture of the outflow tract with the pharyngeal wall. The positive region behind the outflow (arrow) is the SHF. (B) Section of HH12 embryo demonstrating that Nkx2.5 expression is in the ventral pharyngeal mesenchyme (arrow). (C) Higher magnification of area in box in panel B. (D) Expression domain of Nkx2.5 at HH14. The region of the SHF is marked by the arrow. (E) Section of HH14 embryo showing Nkx2.5 expression in the ventral pharyngeal mesenchyme (arrow). (F) Higher magnification of the area in the box in panel E. (G) HH16 embryo demonstrating Nkx2.5 expression is now concentrated in the ventral pharyngeal mesenchyme caudal to the outflow tract. (H) At HH18, expression of Nkx2.5 is limited to the area caudal to the connection of the outflow tract with the ventral pharynx. (I) Transverse section through the caudal outflow tract of HH18 embryo demonstrating Nkx2.5 expression (arrow). PA1 = pharyngeal arch 1, Ph = pharynx, OFT = outflow tract, At = atrium.

mid-portion of the outflow tract, midway between the distal attachment to the pharynx and presumptive right ventricle (Fig. 2C). By 96 h, the DiI-labeled cells were found at the base of the outflow on the left side which after septation, but prior to wedging of the aorta between the atrioventricular valves, becomes the pulmonary side of the outflow (Figs. 2D, E). These data show that cells from the SHF migrate from the ventral pharyngeal mesenchyme into the developing outflow with the right side of the SHF contributing myocardium to the left or future pulmonary side of the outflow. To determine whether cells were moving into the myocardial plane of the outflow tract from areas cranial to and surrounding the outflow tract, we simultaneously labeled the SHF (Fig. 2F, red) and the ventral pharyngeal mesenchyme at the level of arch 1 or 2 (Fig. 2F, green). While the SHF cells began their migration into the outflow tract on the myocardial plane at 24 h, the cells labeled at the level of arch 1 or 2 remained in place or moved into the outflow tract on the endocardial or cardiac jelly tissue planes (Fig. 2G, no green can be seen in the outflow tract). Histological sections show rhodamine labeling on the myocardial plane, although no fluorescein could be detected (Fig. 2H). These results indicate that even though Nkx2.5 is expressed in arches 1 and 2 cranial to the outflow tract at HH14, the only Nkx2.5-expressing cells that contribute to the myocardium after HH14 are derived from the SHF, which is located behind the outflow tract.

Ablation of the right SHF leads to pulmonary atresia

Neural crest ablation interferes indirectly with the addition of the myocardium from the SHF to the outflow; however, it is not known what the direct consequences are to heart development when addition of the SHF-derived myocardium is directly perturbed. In order to further elucidate the contribution of the SHF to the developing heart, we ablated the right side of the SHF in HH14 chick embryos. Using the microinjection techniques developed above, the right side of the SHF was first microinjected with DiI and neutral red to aid targeting of the laser, and then ablated using a pulsed

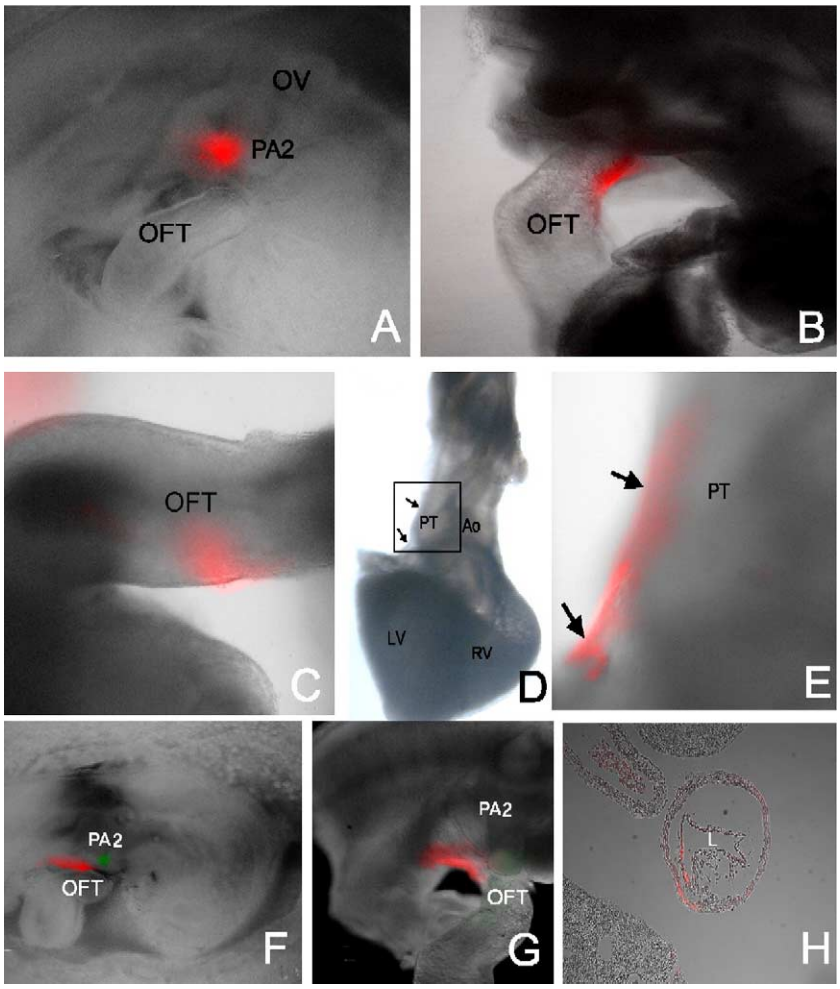

Fig. 2. Right SHF adds to the left side of the preseptation outflow myocardium. Right SHF of HH14 chick embryos labeled with DiI/rhodamine (A) immediately after the injection. (B) 24 h after label of SHF demonstrating movement of cells into outflow tract viewed from the left side. (C) Left view of a heart 48 h after marking showing fluorescent cells now in the mid-portion of the caudal wall of the outflow tract and moving toward the left side. (D) 96 h after labeling, cells are located at base of the outflow on the left side above the left ventricle in this ventral view of the heart. The atria have been removed. (E) Higher magnification of boxed area in panel D to see labeled cells as base of outflow tract. (F) Time 0 of right SHF labeled with DiI/TAMRA-SE (red) and ventral pharyngeal mesenchyme at level of arch 2 labeled with CF-SE (green). (G) 24-h time point of labeling shows the red-labeled SHF adding to the outflow while mesenchyme from arch 2 (green) does not. (H) Section of labeled embryo at the 24-h time point demonstrates red labeling in the myocardial wall but no green-labeled cells have moved into the outflow tract from pharyngeal arch 2. OV = otic vesicle, OFT = outflow tract, PA2 = pharyngeal arch 2, PT = pulmonary trunk, Ao = aorta, LV = left ventricle, RV = right ventricle, L = lumen.

nitrogen-dye laser. In order to confirm the placement of the ablation, we allowed the embryos to incubate for 1 h and then stained with SyTox Green which marks cell necrosis. The necrotic area was found in the ventral pharynx just caudal to the outflow at the level of pharyngeal arch 3, and co-localized with the DiI marking (Fig. 3A). In addition, sections of the Sytox green-stained embryos confirmed that the ablation was in the ventral pharyngeal mesoderm and involved only the right side of the SHF (Fig. 3B). Using the same ablation technique, a series of embryos with SHF ablations were allowed to develop until day 9 and the hearts were harvested for evaluation of gross morphology. Figs. 3C–F depict the variety of phenotypes found. Most commonly, the aorta and pulmonary trunk were oriented in a side-by-side fashion (Fig. 3E), with the aorta to the right of the pulmonary trunk rather than wedged behind it. In the more severe cases, the pulmonary trunk was drastically reduced in size (Fig. 3D) and in some cases completely missing (Fig. 3F). The hearts were then sectioned and stained with H&E or thionine to more accurately assess morphology. Sections revealed ventricular septal defects in the affected hearts (compare Fig. 4B with Figs. 4E, G arrows). The side-by-side orientation of the aorta and pulmonary trunk was more obvious in histological sections (compare Fig. 4C with Fig. 4F). The reduced size of the pulmonary trunk as compared to the aorta was also more apparent (Fig. 4F). Figs. 4G–I represent the most severe phenotype in which there was complete atresia of the pulmonary trunk. Here, the aortic outflow tract formed and communicated with both ventricles by way of a large VSD (Figs. 4J–L). No pulmonary infundibulum was formed, leaving the aorta as the common outflow for both right and left ventricles. The aortic valve was

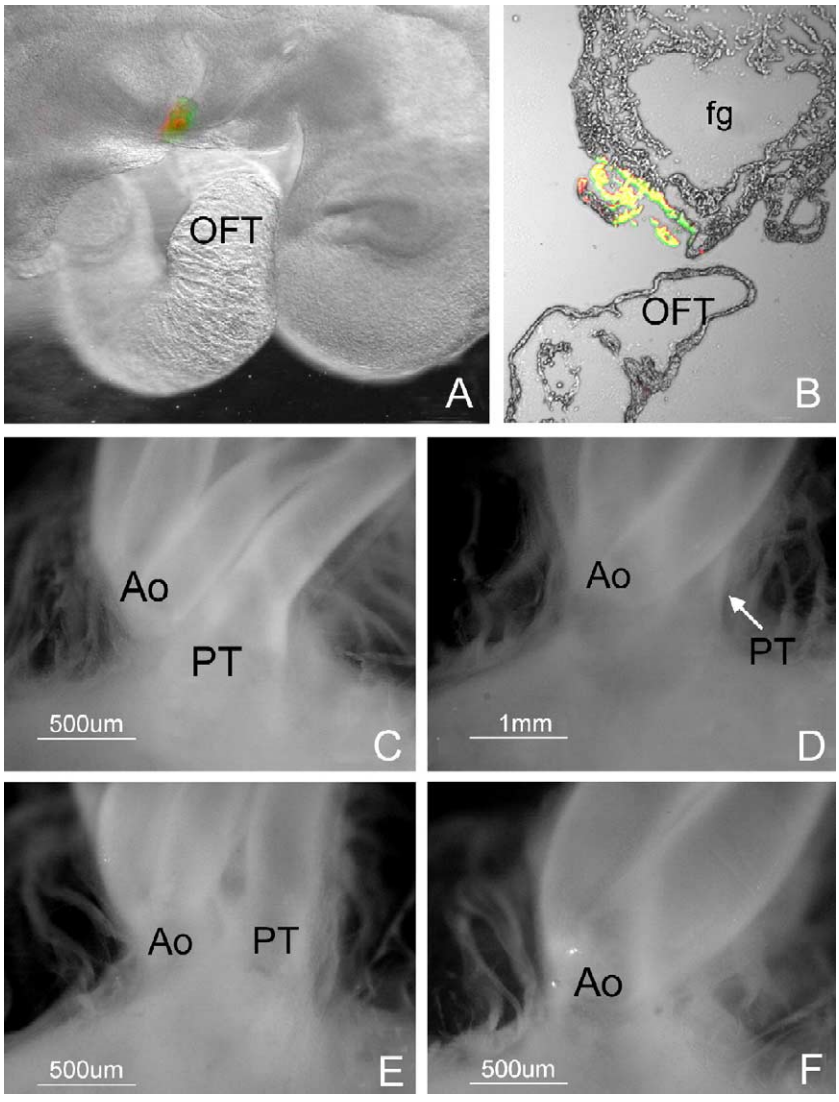

Fig. 3. Ablation of the right SHF results in overriding aorta and pulmonary atresia. (A) Sytox green staining of embryo after laser ablation demonstrating necrosis in the SHF. The red fluorescent DiI label was used to target the laser and can be seen overlapping the green fluorescent necrotic area. (B) Section of the embryo in panel A confirming that necrosis is in the ventral pharyngeal mesenchyme below the foregut (fg) and overlaps with the DiI label (yellow). Note that the ablation only affects the right SHF. (C) Sham-operated embryo demonstrating normal alignment of outflow tract with the pulmonary trunk (PT) located anterior to the aorta (Ao). (D) Right SHF-ablated embryo with side-by-side orientation of the PT and Ao and reduced size of the PT (arrow). (E) Right SHF-ablated embryo with side-by-side orientation of the PT and Ao, demonstrating the overriding aorta. (F) Right SHF-ablated embryo with absent PT.

normally formed with three leaflets, confirming that the malformation is pulmonary atresia and not persistent truncus, since persistent truncus in the chick has four or more leaflets at the ventriculoarterial junction. In total, we found that 76% of embryos were affected by ablation of the SHF: 52% with side-by-side orientation of the aorta and pulmonary trunks, 8% with reduced size of the pulmonary trunk, and 16% with complete pulmonary atresia (Table 1). None of the sham embryos were affected.

The role of the SHF at later stages of development

In situ hybridization indicated that the expression of Nkx2.5 was reduced in the SHF after HH18, and we therefore hypothesized that addition of myocardium by the SHF was complete by this stage of development. We therefore marked the right side of the SHF behind the outflow tract in HH18 embryos and monitored the migration of the cells at 4-h intervals (Fig. 5A). The labeled cells did not progress into the outflow myocardium as seen in labeling experiments done at earlier stages, but instead were found in the caudal wall of the lengthening aortic sac which will contribute to the smooth muscle portion of the outflow vessels above the aortic and pulmonary valves (Fig. 5B) (Waldo et al., 2005a,b). We then ablated the SHF at HH18 using the methods described above. The later ablation of the right SHF did not affect outflow alignment, since the ablated embryos demonstrated appropriate wedging of the aorta behind the pulmonary artery (Figs. 5C–H). These results were not unexpected, since the addition of the early

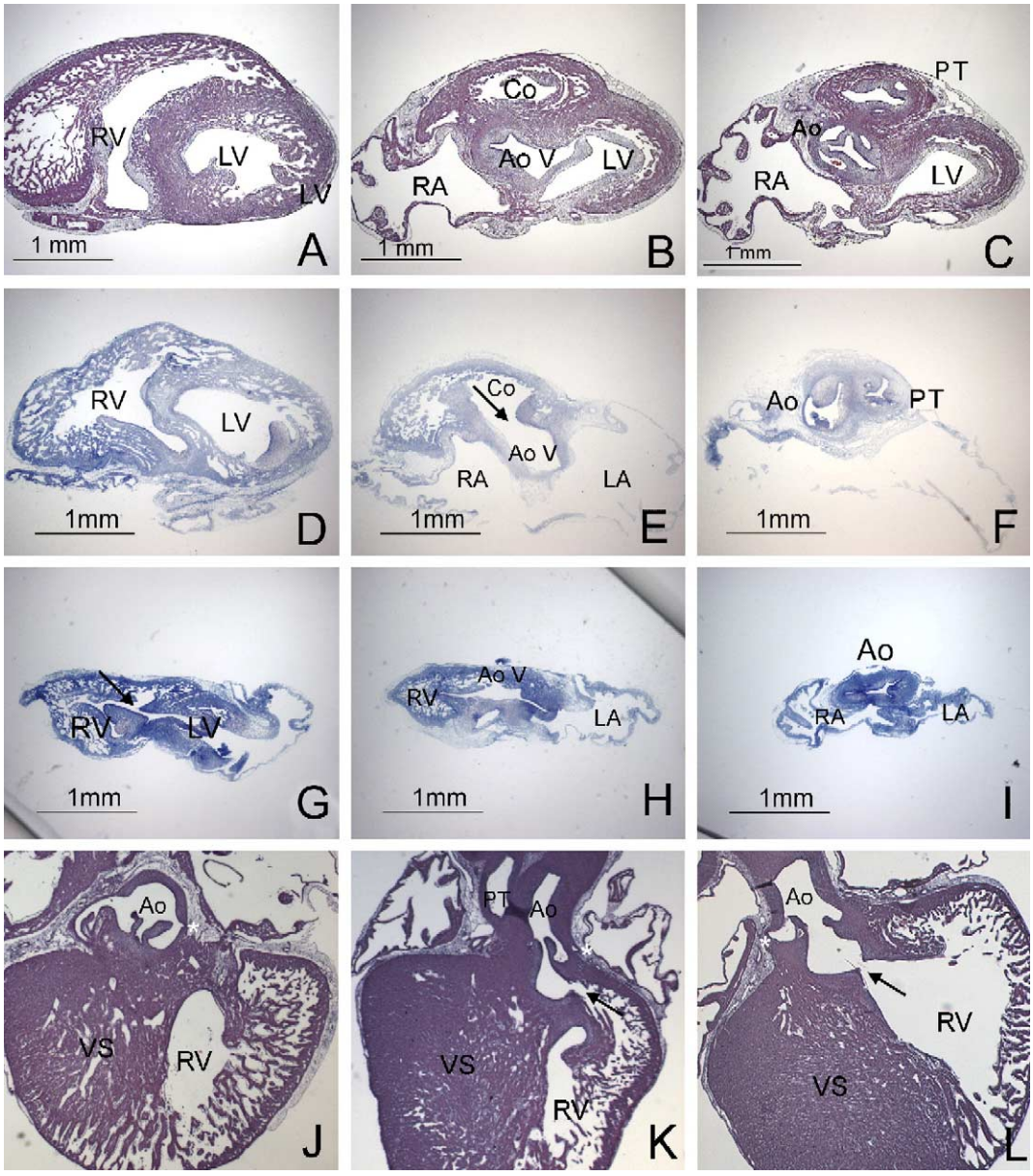

Fig. 4. Histology of right SHF-ablated embryos. (A–C) Serial sections of sham-operated embryo demonstrating normal alignment of the pulmonary and aortic outflow tracts, as well as normal alignment at valve level with the pulmonary trunk (PT) anterior to the aorta (Ao) (C). (D–F) Serial sections of right SHF-ablated embryo with ventricular septal defect (VSD, arrow) and side-by-side orientation of pulmonary and aortic valves (F). (G–I) Serial sections of right SHF-ablated embryo with a VSD (arrow) and an aortic outflow that communicates with both left and right ventricles (H). Note absence of right ventricular outflow tract anterior to aortic outflow. At valve level, the aortic valve forms the only outflow for both ventricles and there is complete pulmonary atresia (I). (J) Frontal section of sham-operated embryo demonstrating how the ventricular septum prohibits communication of the aorta and right ventricle. (K) Frontal section of SHF-ablated embryo with side-by-side orientation to PT and Ao, as well as VSD (arrow) which allows communication of aorta with RV. (L) Frontal section of SHF-ablated embryo with pulmonary atresia and VSD, allowing communication of Ao with RV. In panels J–L, asterisks are used to mark the coronary artery ostia. PT = pulmonary trunk, Ao = aorta, RV = right ventricle, LV = left ventricle, Co = right ventricular conus, Ao V = aortic vestibule, RA = right atrium, LA = eft atrium, VS = ventricular septum.

myocardial component of the SHF, necessary for the lengthening of the outflow and the normal alignment of the outflow with respect to the ventricles, was not disturbed.

Coronary artery anomalies after ablation of the SHF

The insertion of the coronary arteries into the aorta was normal in embryos ablated at stage 14 that were only moderately affected with side-by-side orientation to the outflow vessels (data not shown). However, in the more severely affected hearts, coronary artery anomalies were present (Fig. 6). Similar coronary anomalies were seen in the embryos ablated at HH18, despite the fact that the aorta and pulmonary trunk showed correct alignment (Figs. 5E–H). The coronary anomalies seen included: two coronaries originating from a single cusp (Fig. 6C), two coronaries

Table 1
Summary of cardiovascular phenotypes in embryos with secondary heart field ablations

	Sham (%)	Ablated (%)
Affected	0	19 (76)
Overriding aorta		13 (52)
Pulm stenosis		2 (8)
Pulm atresia		4 (16)
Normal	100	6 (24)

originating from a single ostium (Figs. 5G, H), and absence of either one or both coronary artery stems (Figs. 5E, F, and 6D, respectively). In the embryos with absent coronary stems, multiple small endothelial channels were seen on the periphery of the aorta (Fig. 6D, arrowheads). The identity of these channels as endothelial in origin was confirmed by staining with factor-VIII-related antigen, which marks the endothelium of blood vessels in chick embryos starting at day 8 of development (Figs. 6E–G) (Ribatti et al., 1999). Coronary artery development in chick embryos occurs as subepicardial endothelial channels grow into the aorta from a ring of capillaries that surrounds the outflow vessels. These channels eventually grow through the aortic wall to become the coronary stems by day 7 of chick development (Waldo et al., 1994). In the SHF-ablated embryos with absent coronary stems, these endothelial channels were indeed present at day 9 (Fig. 6D, arrowheads) but did not form the coronary stems. Thus, these data suggest that, without the addition of the smooth muscle component from the SHF, these endothelial channels were unable to appropriately target the right and left coronary sinuses of the aorta and to form right and left coronary stems. Further,

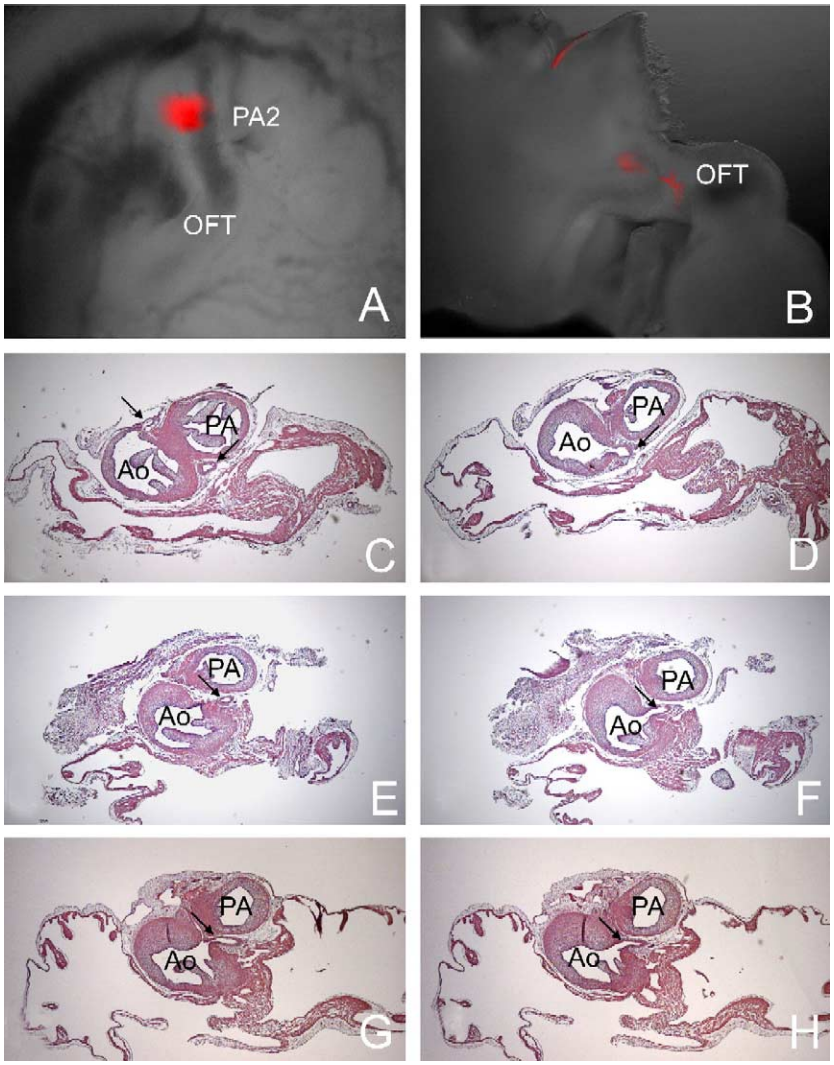

Fig. 5. SHF ablations at HH18 have normal outflow alignment but coronary artery anomalies. (A) SHF labeling with DiI/fluorescein in HH18 embryo at time 0. The labeled cells were located in the region caudal to the outflow in the region of the 3rd arch. (B) 24 h after the injection, the cells have moved into the caudal wall of the aortic sac (view of the right side). (C, D) Sham-operated embryo demonstrating normal alignment of the aorta and pulmonary trunk and normal placement of the coronary artery stems (black arrows). (E, F) Embryo with right SHF ablated at HH18 shows normal alignment of the pulmonary trunk and aorta. The aorta has a single coronary artery (black arrow). (G, H) Embryo with right SHF ablated at HH18 and normal outflow tract alignment but both coronaries originate from a single ostium (black arrow). PA = pulmonary artery, Ao = aorta.

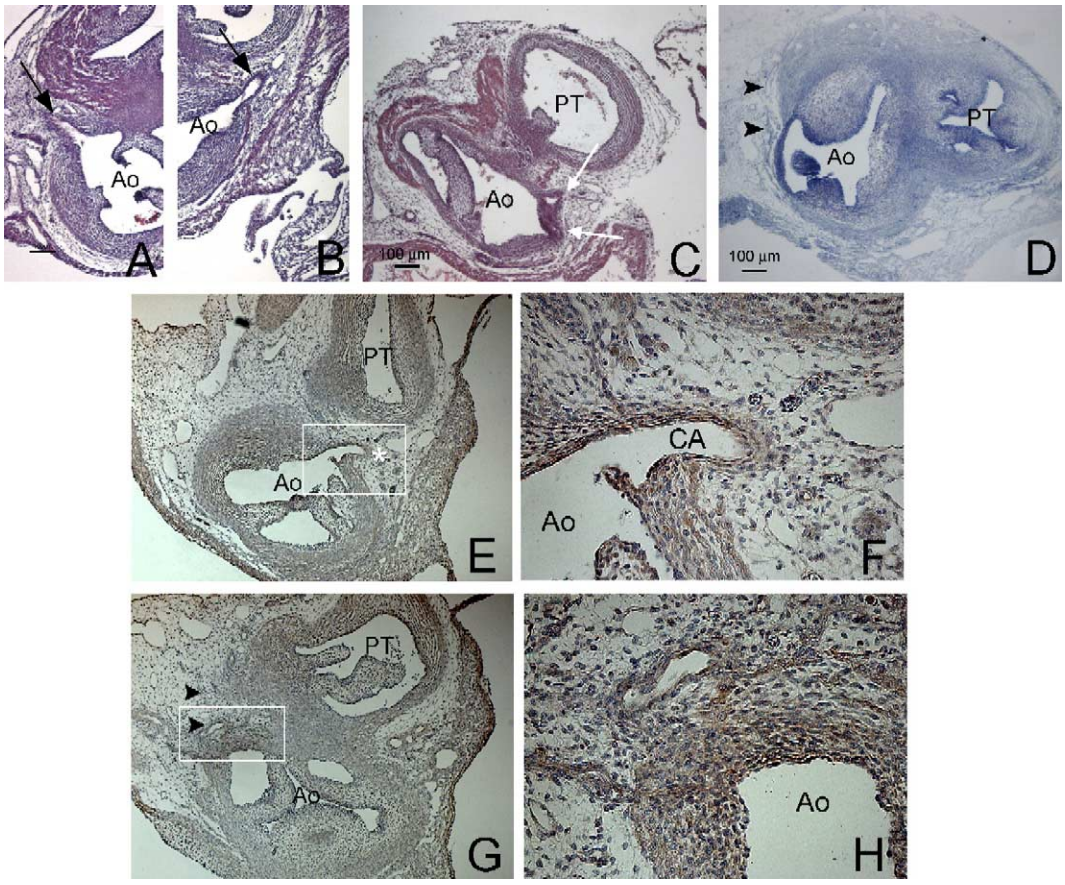

Fig. 6. Coronary anomalies in SHF-ablated embryos. (A, B) Sections of sham-operated embryo demonstrating normal coronary stems on the right and left sides of the aorta (black arrows). (C) SHF-ablated embryo with both coronary stems from a single sinus. (D) Same embryo as shown in Figs. 4D–F showing absence of coronary stems. Arrowheads mark coronary capillary network surrounding the base of the aorta. (E) SHF-ablated embryo stained with antibody to factor-VIII-related antigen, which marks the endothelium. Asterisk marks coronary stem from the left sinus. Note absence of coronary on right side. (F) Higher magnification of area indicated in panel E showing coronary stem with positive factor-VIII-related antigen staining (brown). (G) Same embryo as shown in panels E and F demonstrating coronary capillary network (arrowheads) surrounding the base of the aorta on the right. Note the presence of the coronary seen on left side (asterisk in E) and absence of coronary capillary network on left side in F. (H) Higher magnification of area indicated in panel G demonstrating capillary network seen with positive staining of antibody to factor-VIII-related antigen (brown), confirming its endothelial identity. Ao = aortic valve, PT = pulmonary trunk, CA = coronary artery.

since the majority of coronary anomalies were present in embryos in which the ablations were performed at HH18, it appears that the later addition of the smooth muscle cells from the SHF to the caudal wall of the aortic sac is important for coronary artery development.

Discussion

The present study outlines two roles for the SHF in outflow tract development. At early stages, the SHF is responsible for the addition of myocardium to lengthen the myocardial outflow tract as our DiI/rhodamine labeling studies document the movement of cells from the SHF into the outflow and their migration toward the right ventricle. This additional myocardium elongates the outflow and provides length for appropriate looping. It also adds spiraling myocardium that may accommodate the rotation required for appropriate alignment of the aorta and pulmonary trunk with the left and right ventricles. During the process of wedging, the aortic valve rotates behind the pulmonary trunk and settles between the two atrioventricular valves. In both neural-crest- and SHF-ablated embryos, disrupted addition of the SHF results in malalignment of the cardiac outflow tract. In the SHF-ablated embryos, the lack of addition of the SHF-derived myocardium results in a shorter outflow that cannot undergo rotation. Since septation is normal, this results in an overriding aorta and side-by-side orientation of the aorta and pulmonary trunk. Similarly, in the neural-crest-ablated embryos, the SHF is not added and outflow rotation does not occur; however, without neural crest cells, the phenotype is additionally complicated by lack of outflow septation, leading to a malaligned PTA. The present study and that by Yelbuz et al. (2002) and Waldo et al. (2005a,b) demonstrate that, in both cases, the defects in cardiac outflow alignment are the result of disrupted addition of the myocardium from the SHF. Another model of tetralogy of Fallot has been created in chick by Watanabe

and colleagues by preventing cell death in the outflow myocardium as it is absorbed into the right ventricle (Watanabe et al., 1998, 2001). Thus, both the generation and remodeling of the outflow myocardium are critical to proper alignment of the ventriculoarterial connection and wedging of the aorta. In addition, defects high in the ventricular septum were present in many of the embryos that underwent SHF ablation. While these VSDs may occur secondary to developmental pressures on the embryo from the defects in outflow alignment, they may also be part of the phenotype itself. We hypothesize that the secondary heart field may contribute the myocardium necessary to form the highest portion of the ventricular septum which is directly connected to the great vessels. Also, the VSD could result from an unbridgeable gap resulting from the malalignment itself, since the outflow tract is not appropriately positioned over the future right and left ventricles for ventricular septal closure.

Our study also demonstrates that the myocardial addition of the SHF takes place with a specific geometry in that the right side spirals behind and into the left side of the outflow tract. In the preseptation outflow tract, this represents the future pulmonary outflow. It is not surprising, therefore, that the ablation of the right SHF results in disruption of development of the right ventricular outflow and pulmonary trunk, either by reduction in size of the pulmonary outflow (pulmonary stenosis) or complete pulmonary atresia. We therefore hypothesize that the left side of the SHF adds to the right side of the developing outflow and that ablation of this side would lead to aortic stenosis or atresia. However, testing this hypothesis will be difficult since the chick embryo lies on its left side.

Nkx2.5 expression in the myocardial precursors in the pharynx is greatly reduced by HH18, suggesting that addition of myocardial precursor cells from the SHF is complete by this stage. Although DiI/rhodamine labeling experiments done at this later stage did demonstrate movement of the SHF into the arterial pole, the cells did not end up in the myocardium of the outflow tract. Instead, they incorporated themselves into the caudal wall of the aortic sac. This portion of the aortic sac will later make up the vascular smooth muscle component of the outflow vessels above the pulmonary and aortic valves (Fig. 6B and Waldo et al., 2005a,b). Interestingly, it has been known for many years that the tunica media contributed by the cardiac neural crest ended at some distance above the valve, and the source of the non-neural crest-derived vascular smooth muscle at the base of the aorta and pulmonary trunk has been unclear (Fig. 7). We now believe that the SHF is responsible for this area of smooth muscle above the aortic and pulmonary valves, and that this smooth muscle component is added after the myocardial addition is complete (Waldo et al., 2005a,b). This hypothesis is supported by the ablation of the SHF at HH18, since these embryos do not manifest problems with cardiac outflow alignment but do have defects in the non-neural crest-derived smooth muscle region.

Our data also demonstrate that the successful addition of the SHF is required for correct formation of the coronary arteries, since coronary artery anomalies are seen after both the HH14 and 18 ablations. In the embryos ablated at HH14, coronary artery anomalies are seen only in the most severely affected embryos, indicating a more complete ablation of both the early and the late components of the SHF in these embryos. In the embryos ablated at HH18, only the later component of SHF addition to the aortic sac is affected. Since the later cells added from the SHF to the aortic sac provide vascular smooth muscle at the base of the outflow vessels, these experiments suggest that this later addition of SHF to the aortic sac is required for appropriate targeting of the coronary stems to the right and left coronary sinuses.

Thus, our work demonstrates that the SHF participates in development of the cardiac outflow tract in two fundamental ways. First, the SHF contributes cells to the myocardial wall

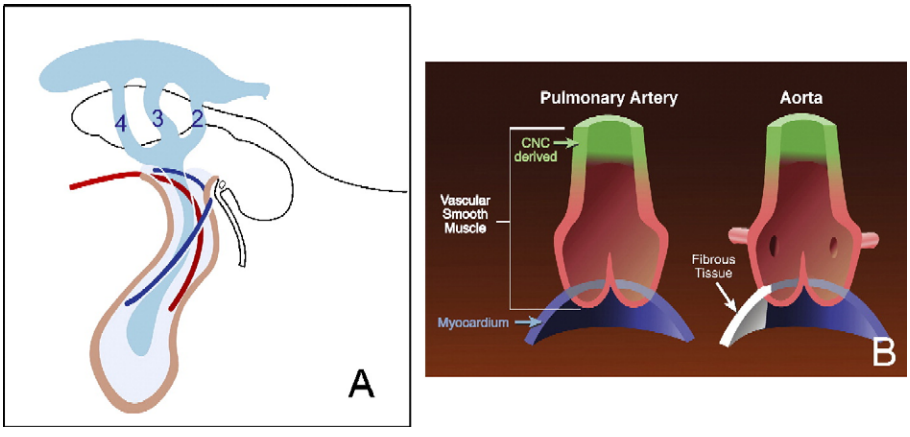

Fig. 7. Model of addition of SHF. (A) Myocardium from the right SHF (red) spirals behind outflow and to the left side of the preseptation outflow myocardium which will become the pulmonary side of the outflow. Blue represents the putative path of the left SHF anterior and to the right base of the outflow. (B) SHF adds a myocardial component to the outflow tract (blue) and subsequently contributes the vascular smooth muscle above the outflow valves (red) and below the cardiac neural-crest-derived tunica media (green).

prior to HH18. This myocardium is added in a spiral with right SHF contributing to the back and left side of the outflow (Fig. 7A). After HH18, the SHF contributes to the caudal wall of the aortic sac which is not added in a spiral and will later become the vascular smooth muscle of the outflow vessels above the valve. The two components added to the outflow tract by the SHF together form the myocardial/smooth muscle transition that occurs at the level of the aortic and pulmonary valves (Fig. 7B). If both components of the SHF are not added correctly, this transition is disrupted. Our experiments suggest that the coronaries require the later addition from the right SHF to appropriately target their insertion into the aorta as ablation of the right SHF at HH18 results in coronary artery defects. However, it is also possible that the coronaries use the myocardial/smooth muscle boundary to find their insertion site into the aorta, and that the disruption of this boundary leads to coronary artery anomalies.

Finally, the developmental defects seen after SHF ablation (coronary artery anomalies, overriding aorta, and pulmonary stenosis or atresia) are major components of certain conotruncal heart defects, namely, double outlet right ventricle and tetralogy of Fallot (Table 1). These abnormalities are also seen after neural crest ablation and represent major components of the DiGeorge phenotype in humans. One of the underlying genetic disturbances in the DiGeorge phenotype is microdeletion of chromosome 22q11. In fact, the prevalence of 22q11 deletions among patients with tetralogy of Fallot is much higher in patients with pulmonary atresia than in patients with tetralogy of Fallot alone (Gelb, 1997). *TBX1*, a transcription factor identified in the 22q11 region, is thought to be the major determinant of the DiGeorge phenotype, since *TBX1* mutations recapitulate the syndrome in mice. Recent work by Xu et al. demonstrated that conditional deletion of *TBX1* resulted in decreased cell proliferation in the secondary heart field and that this occurred by a cell non-autonomous mechanism (Xu et al., 2004). This work in conjunction with the present study furthers the notion that tetralogy of Fallot and double outlet right ventricle represent a subset of congenital heart disease caused by defects in the secondary heart field, since they can be recreated both mechanically and genetically.

Point mutations in Nkx2.5 are also associated with tetralogy of Fallot and pulmonary atresia in humans (Benson et al., 1999; Goldmuntz et al., 2001). Teratogenic and genetic models of tetralogy of Fallot and pulmonary atresia have been described. Nitrofen induces many of the defects in rats that are also seen in the DiGeorge phenotype including tetralogy of Fallot and pulmonary atresia. Nitrofen also causes congenital diaphragmatic hernia (Kim et al., 1999; Losty et al., 1999). Interestingly, the splanchnic mesoderm that forms the SHF in the ventral pharynx is directly continuous with the somatic mesoderm that forms the diaphragm, suggesting a link between these two mesodermal fields.

Our results suggest for the first time that tetralogy of Fallot and pulmonary atresia represent the clinical manifestation of disrupted addition of the SHF and indicate an important role for the SHF in understanding the embryogenesis of these diseases.

Acknowledgments

We thank Karen Waldo for preparing illustrations, Karen Waldo, Erik Meyers, and Tony Creazzo for valuable discussions of the data, and Tony Creazzo for comments on the manuscript. This work was supported by PHS grants HL070140, HD39946, and HL36059 to MLK and a Sarnoff Foundation Investigator Award to CW.

References

Benson, D.W., Silberbach, G.M., Kavanaugh-McHugh, A., Cottrill, C., Zhang, Y., Riggs, S., Smalls, O., Johnson, M.C., Watson, M.S., Seidman, J.G., Seidman, C.E., Plowden, J., Kugler, J.D., 1999. Mutations in the cardiac transcription factor NKX2.5 affect diverse cardiac developmental pathways. J. Clin. Invest. 104, 1567–1573.

Cai, C., Liang, X., Shi, Y., Chu, P.-H., Pfaff, S.L., Chen, J., Evans, S., 2003. Isl1 identifies a cardiac progenitor population that proliferates prior to differentiation and contributes a majority of cells to the heart. Dev. Cell 5, 877–899.

Farrell, M., Waldo, K., Li, Y.X., Kirby, M.L., 1999a. A novel role for cardiac neural crest in heart development. Trends Cardiovasc. Med. 9, 214–220.

Farrell, M.J., Stadt, H., Wallis, K.T., Scambler, P., Hixon, R.L., Wolfe, R., Leatherbury, L., Kirby, M.L., 1999b. HIRA, a DiGeorge syndrome candidate gene, is required for cardiac outflow tract septation. Circ. Res. 84, 127–135.

Farrell, M.J., Burch, J.L., Wallis, K., Rowley, L., Kumiski, D., Stadt, H., Godt, R.E., Creazzo, T.L., Kirby, M.L., 2001. FGF-8 in the ventral pharynx alters development of myocardial calcium transients after neural crest ablation. J. Clin. Invest. 107, 1509–1517.

Gelb, B.D., 1997. Molecular genetics of congenital heart disease. Curr. Opin. Cardiol. 12, 321–328.

Goldmuntz, E., Geiger, E., Benson, D.W., 2001. NKX2.5 mutations in patients with tetralogy of fallot. Circulation 104, 2565–2568.

Hamburger, V., Hamilton, H.L., 1951. A series of normal stages in the development of the chick embryo. J. Morphol. 88, 49–92.

Kelly, R.G., Brown, N.A., Buckingham, M.E., 2001. The arterial pole of the mouse heart forms from Fgf10-expressing cells in pharyngeal mesoderm. Dev. Cell 1, 435–440.

Kim, W.G., Suh, J.W., Chi, J.G., 1999. Nitrofen-induced congenital malformations of the heart and great vessels in rats: an animal model. J. Pediatr. Surg. 34, 1782–1786.

Kirby, M.L., Gale, T.F., Stewart, D.E., 1983. Neural crest cells contribute to aorticopulmonary septation. Science 220, 1059–1061.

Losty, P.D., Connell, M.G., Freese, R., Laval, S., Okoye, B.O., Smith, A., Kluth, D., Lloyd, D.A., 1999. Cardiovascular malformations in experimental congenital diaphragmatic hernia. J. Pediatr. Surg. 34, 1203–1207.

Mjaatvedt, C.H., Nakaoka, T., Moreno-Rodriguez, R., Norris, R.A., Kern, M.J., Eisenberg, C.A., Turner, D., Markwald, R.R., 2001. The outflow tract of the heart is recruited from a novel heart-forming field. Dev. Biol. 238, 97–109.

Ribatti, D., Nico, B., Vacca, A., Ronacali, L., 1999. Localization of factor VIII-related antigen in the endothelium of the chick embryo chorioallantoic membrane. Histochem. Cell Biol. 112, 447–450.

Waldo, K.L., Kumiski, D.H., Kirby, M.L., 1994. Association of the cardiac neural crest with development of the coronary arteries in the chick embryo. Anat. Rec. 239, 315–331.

Waldo, K.L., Kumiski, D., Kirby, M.L., 1996. Cardiac neural crest is essential for the persistence rather than the formation of an arch artery. Dev. Dyn. 205, 281–292.

Waldo, K., Miyagawa-Tomita, S., Kumiski, D., Kirby, M.L., 1998. Cardiac neural crest cells provide new insight into septation of the cardiac outflow tract: aortic sac to ventricular septal closure. Dev. Biol. 196, 129–144.

Waldo, K.L., Kumiski, D.H., Wallis, K.T., Stadt, H.A., Hutson, M.R., Platt, D.H., Kirby, M.L., 2001. Conotruncal myocardium arises from a secondary heart field. Development 128, 3179–3188.

Waldo, K.L., Hutson, M.R., Zdanowicz, M., Stadt, H.A., Kumiski, D., Abu-Issa, R., Kirby, M.L., 2005a. Secondary heart field contributes myocardium and smooth muscle to the arterial pole of the developing heart. Dev. Biol. 281, 78–90.

Waldo, K., Hutson, M.R., Zdanowicz, M., Stadt, H.A., Zdanowicz, J., Kirby, M.L., 2005b. Cardiac neural crest is necessary for normal addition of the myocardium to the arterial pole from the secondary heart field. Dev. Biol. 281, 66–77.

Watanabe, M., Choudhry, A., Berlan, M., Singal, A., Siwik, E., Mohr, S., Fisher, S.A., 1998. Developmental remodeling and shortening of the cardiac outflow tract involves myocyte programmed cell death. Development 125, 3809–3820.

Watanabe, M., Jafri, A., Fisher, S.A., 2001. Apoptosis is required for the proper formation of the ventriculo-arterial connections. Dev. Biol. 240, 274–288.

Wilkinson, D.G., 1992. In situ hybridization. In: Rickwood, D., Hames, B.D. (Eds.), In in Situ Hybridization: A Practical Approach. IRS Press, Oxford, pp. 75–83.

Xu, H., Morishima, M., Wylie, J.N., Schwartz, R.J., Bruneau, B., Lindsay, E.A., Baldini, A., 2004. Tbx1 has a dual role in the morphogenesis of the cardiac outflow tract. Development 131, 3217–3227.

Yelbuz, T.M., Waldo, K.L., Kumiski, D.H., Stadt, H.A., Wolfe, R.R., Leatherbury, L., Kirby, M.L., 2002. Shortened outflow tract leads to altered cardiac looping after neural crest ablation. Circulation 106, 504–510.